

**SEISMIC CHARACTERIZATION OF NORTHEAST ASIA**

Kevin Mackey<sup>1</sup>, Lee Steck<sup>2</sup>, Kazuya Fujita<sup>1</sup>, Hans Hartse<sup>2</sup>, and Richard Stead<sup>2</sup>

Michigan State University<sup>1</sup> and Los Alamos National Laboratory<sup>2</sup>

Sponsored by National Nuclear Security Administration

Contract Nos. DE-FC52-2004NA25540<sup>1</sup> and DE-AC52-06NA25396<sup>2</sup>

**ABSTRACT**

Our project of seismic characterization of northeast Asia has continued on a multi-faceted approach concentrating on eastern Russia, including field deployments, data synthesis and interpretation, database integration, and travel-time tomography.

For field efforts, we deployed four remote seismic stations in the Seimchan-Buyunda basin in the Magadan region to get a better idea of baseline seismicity. Several events per day were recorded over approximately 40 days of station operation; the detection threshold for events was an order of magnitude higher than that of base stations in the cities. Suspected faulting-related geomorphological features observed in satellite images were also field checked along the Ulakhan Fault, a major earthquake generating feature, in this area. Fault scarps and sag ponds were identified cutting across a major alluvial fan. These dramatic features were previously undocumented and represent part of a major, but poorly understood fault system. This fault likely represents ground truth locations of earthquakes in the area.

For data analysis efforts, we completed interpretation of earthquake records from seismic stations deployed in the Stanovoi Range in 2006, including the determination of a composite focal mechanism. Other data analysis included extending our focal mechanism compilation of eastern Siberia to northeast Kamchatka, and analysis of seismicity and mechanisms in the Karaginsky Island area. Finally, we also updated focal mechanism and seismicity compilations for the Chersky Range.

Our Siberia database enhancements for this past year include: (1) addition of new origin information for earthquakes and explosions (and associated phase data and amplitudes), from the Irkutsk, Yakutsk, and Magadan networks., (2) additional catalog information from Siberia and the Far East in Russian language (Cyrillic) spread sheets covering years 1998-2004, and (3) and the inclusion of United States Geological Survey Earthquake Data Reports and International Seismological Centre magnitudes for larger events where Russian network operators did not report a K-class or a magnitude estimate.

We have been using Pn, Pg, and Lg tomography to obtain crustal and upper-mantle velocities in northeast Asia. Pn velocities are higher beneath the Siberian Platform and generally lower under the tectonically active regions in the central and eastern portions of our study area. Pg velocities show a similar geographic trend, and our results agree closely with Pg results from earlier studies. Pg velocities beneath Sakhalin Island are anomalously low and we are working to understand this observation. Lg velocities are high beneath the Siberian Platform, the Chersky Range and the Verkhoyansk Foldbelt. Low Lg velocities are found beneath Sakhalin Island. In general, average Vp/Vs ratios of 1.73 to 1.75 are found throughout the study region. Travel-time correction surfaces will be developed from the tomographic maps, and these will be compared to correction surfaces currently being developed from the raw travel-time data.

# Report Documentation Page

Form Approved  
OMB No. 0704-0188

Public reporting burden for the collection of information is estimated to average 1 hour per response, including the time for reviewing instructions, searching existing data sources, gathering and maintaining the data needed, and completing and reviewing the collection of information. Send comments regarding this burden estimate or any other aspect of this collection of information, including suggestions for reducing this burden, to Washington Headquarters Services, Directorate for Information Operations and Reports, 1215 Jefferson Davis Highway, Suite 1204, Arlington VA 22202-4302. Respondents should be aware that notwithstanding any other provision of law, no person shall be subject to a penalty for failing to comply with a collection of information if it does not display a currently valid OMB control number.

1. REPORT DATE <b>SEP 2008</b>		2. REPORT TYPE		3. DATES COVERED <b>00-00-2008 to 00-00-2008</b>	
4. TITLE AND SUBTITLE <b>Seismic Characterization of Northeast Asia</b>				5a. CONTRACT NUMBER	
				5b. GRANT NUMBER	
				5c. PROGRAM ELEMENT NUMBER	
6. AUTHOR(S)				5d. PROJECT NUMBER	
				5e. TASK NUMBER	
				5f. WORK UNIT NUMBER	
7. PERFORMING ORGANIZATION NAME(S) AND ADDRESS(ES) <b>Michigan State University, East Lansing, MI, 48824</b>				8. PERFORMING ORGANIZATION REPORT NUMBER	
9. SPONSORING/MONITORING AGENCY NAME(S) AND ADDRESS(ES)				10. SPONSOR/MONITOR'S ACRONYM(S)	
				11. SPONSOR/MONITOR'S REPORT NUMBER(S)	
12. DISTRIBUTION/AVAILABILITY STATEMENT <b>Approved for public release; distribution unlimited</b>					
13. SUPPLEMENTARY NOTES <b>Proceedings of the 30th Monitoring Research Review: Ground-Based Nuclear Explosion? Monitoring? Technologies, 23-25 Sep 2008, Portsmouth, VA sponsored by the National Nuclear Security Administration (NNSA) and the Air Force Research Laboratory (AFRL)</b>					
14. ABSTRACT <b>see report</b>					
15. SUBJECT TERMS					
16. SECURITY CLASSIFICATION OF:			17. LIMITATION OF ABSTRACT	18. NUMBER OF PAGES	19a. NAME OF RESPONSIBLE PERSON
a. REPORT	b. ABSTRACT	c. THIS PAGE			
<b>unclassified</b>	<b>unclassified</b>	<b>unclassified</b>	<b>Same as Report (SAR)</b>	<b>10</b>	

**OBJECTIVES**

The main objective of our research is to improve the overall seismic characterization of northeastern Asia. To accomplish this we seek to develop a complete seismicity database and to use this database to discriminate industrial explosions, develop velocity models, and understand the relationship between the sizes, sources (both seismologic character and tectonics), and locations of events.

**RESEARCH ACCOMPLISHED**

**Source Characteristics and Active Faulting.** Understanding the exact location and character of faults is beneficial for ground truth (GT) studies as it makes it possible for events to be tied to specific faults, as well as to understand expected event types. The source characteristics of earthquakes in northeastern Asia have generally been poorly determined. In certain areas (northeast Kamchatka, Stanovoi Range, central Chersky Range), several events have occurred since the general application of centroid moment tensor (CMT) analysis; in others no sizable events have occurred. While the general stress regime has been known for several decades (e.g., Cook et al., 1986; Parfenov et al., 1988), the details in many areas remain unclear. We discuss several aspects of active faulting and source characterization in eastern Russia.

The Ulakhan fault is the primary candidate fault for the edge of the North American plate in eastern Yakutia and the Magadan region (Figure 1) and thus can be expected to be one of the primary active faults in the region. The fault can be traced for nearly 900 km, extending from northwest of the Indigirka River in the north to the southern end of the Seimchan-Buyunda Basin in the south; it is nearly comparable in length to the San Andreas fault. Although most of the Ulakhan fault has never been surveyed on the ground, much of the fault is very clear on satellite images, where clear scarps, offset rivers, sag ponds, etc., are apparent (Figure 2). Geomorphology and consistent offsets in the river drainage system indicate a minimum left-lateral movement along the fault of about 24 km (Fujita et al., 2004) since the river network was established in about the Pliocene. Focal mechanisms also indicate a left-lateral motion on the fault. Analysis of the northern section of the primary branch of the Ulakhan fault shows a series of en-echelon basins in the vicinity of, and west of, the Indigirka River. The Indigirka River, other rivers, geology, and topography all reflect the proposed 24-km left-lateral offset. In Figure 3, we show two images of the northern section of the Ulakhan fault. The upper image is the present day, while the lower shows restored topography and alignment of rivers after cutting the image and removing 24 km of offset. Note that on the restored image, it is difficult to see the cut used for the restoration as river valleys, topography, and rock structure match almost perfectly.

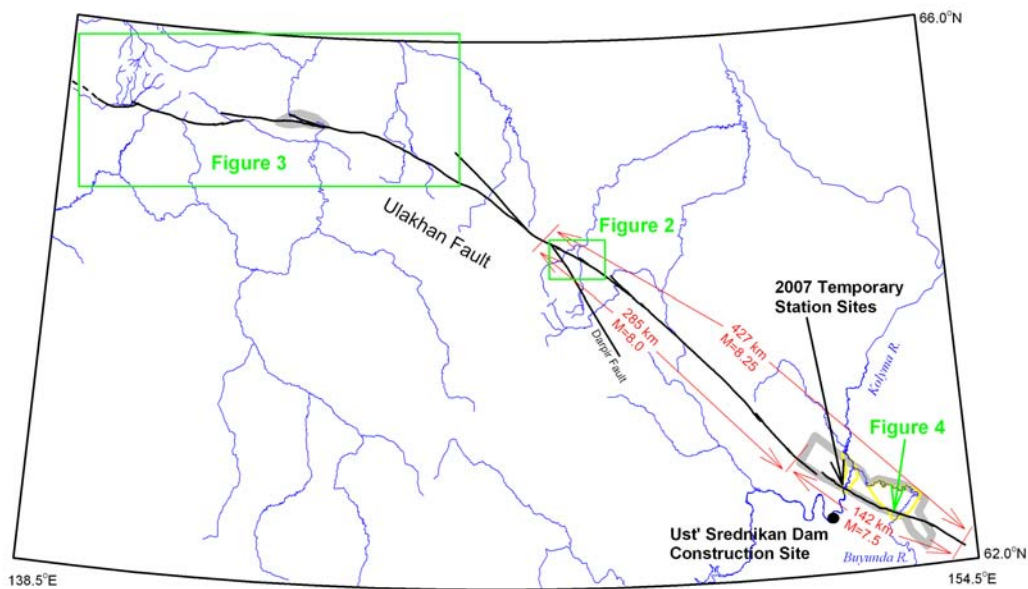


**Figure 1. The Ulakhan fault in the Magadan and Yakutsk regions. Figures as described in the text and below are indicated in green. Red indicates possible fault segments and expected magnitudes if the entire segment slips. The grey region indicates the Seimchan-Buyunda Basin.**

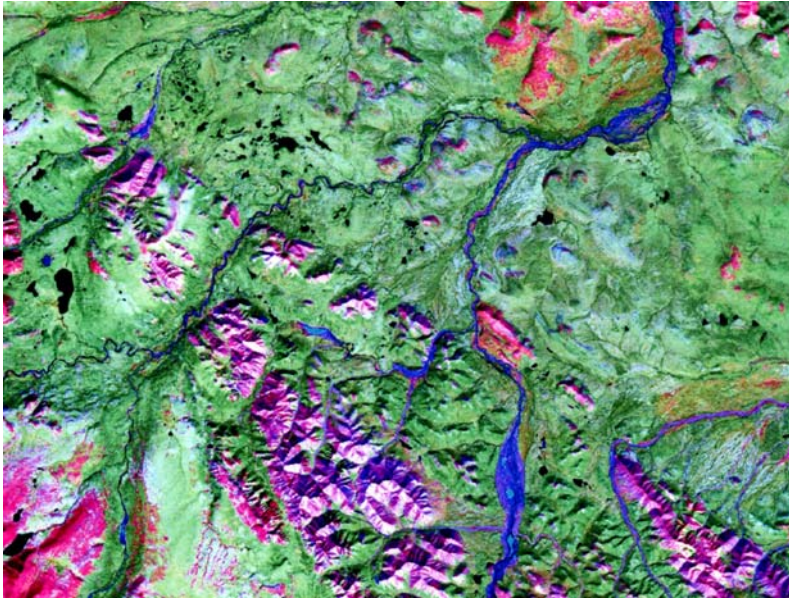


Figure 2. Satellite image of the central Ulakhan fault. The fault extends from upper left to lower right. Note the clear lineation, scarps, offset rivers, and abandoned stream channels.

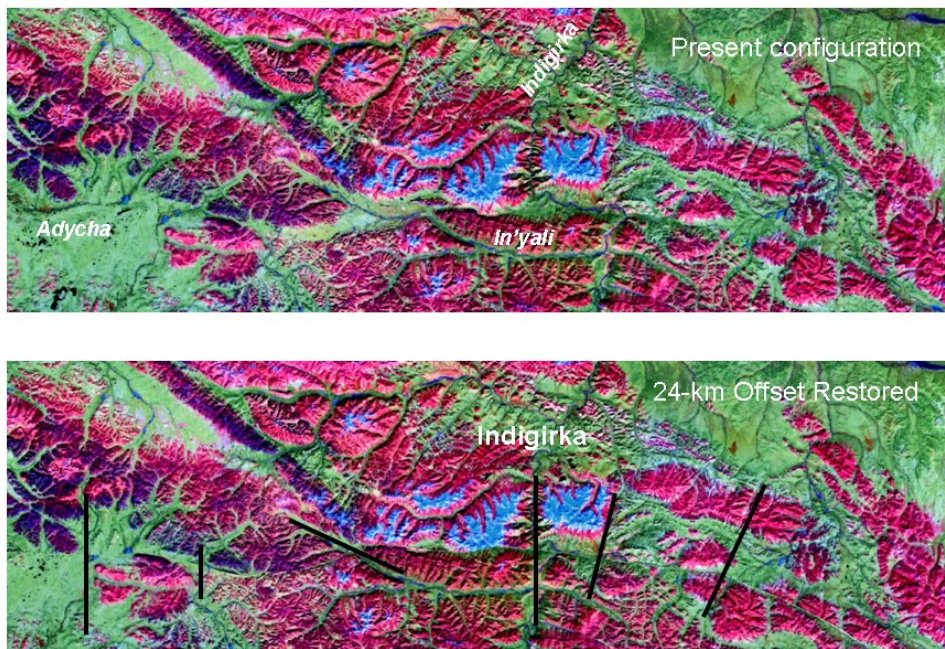
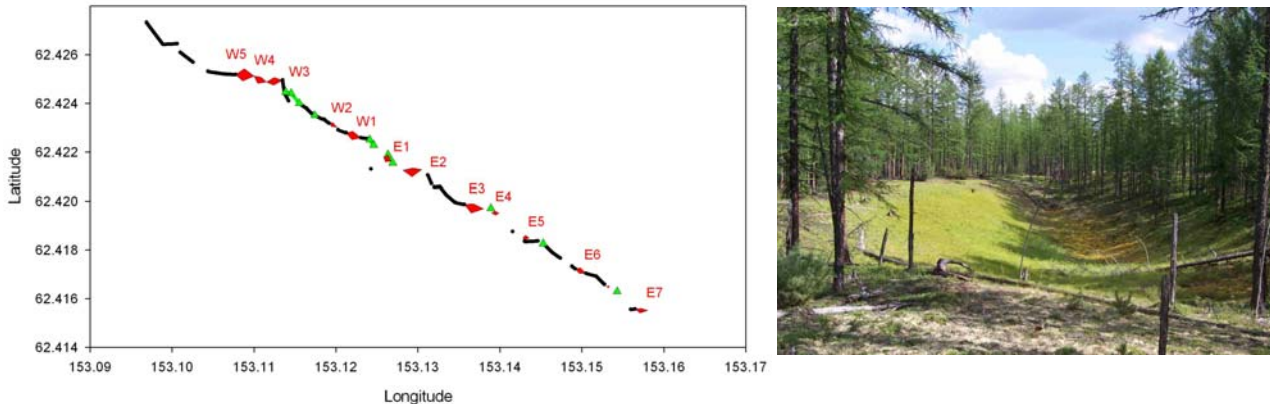


Figure 3. The northern section of the Ulakhan fault in the Yakutsk region. The upper image is the present day, while the lower shows restored topography and alignment of rivers after cutting the image and removing 24 km of offset. Black lines indicate areas of river/valley alignment after restoration.

We surveyed a section of the Ulakhan fault in the southern portion of the Seimchan-Buyunda Basin, where the fault crosses the abandoned alluvial fan of the Buyunda River. Along a 4-km section of the fault, we found a series of 12 well-developed sags connected by pressure ridges and/or scarps (Figure 4a). The scarps have a maximum of about 3 m of vertical offset, with the basin (north) side being lower. We also note that the sags axes are preferentially oriented slightly more east-west than the sections defined by scarps or pressure ridges, consistent with left-lateral motion on the fault. Figure 4b shows one of the well-developed sags. The observed geomorphology is

consistent with the Ulakhan being a significant Strike-Slip fault system. Given the observed fault length, the Ulakhan may be capable of generating great earthquakes. Using relationships proposed by Wells and Coppersmith (1994), the southern segments of the Ulakhan fault may be capable of generating earthquakes in the Magnitude-8 range (Figure 1). It must be stated, however, that the true character of ruptures on the Ulakhan is unknown. No research has been conducted to establish if the fault slips in large, but infrequent, earthquakes, nor what the recurrence interval might be. Seismic hazards on the Ulakhan fault are of particular importance to the Ust' Srednikan Hydroelectric dam on the Kolyma River that is under construction only 27 km from the fault. Additional seismicity studies, field surveys, and geologic research must be conducted to understand the Ulakhan fault and the seismic characteristics of the area.



**Figure 4. A.) Survey of a 4 km section of the Ulakhan fault crossing the alluvial fan of the Buyunda River in the Seimchan-Buyunda Basin. Sags are shown in red, pressure ridges in green and scarps in black (left). B.) Photo of well-developed sag E7 on A (right).**

We conducted a small seismic deployment in the Seimchan Basin along the Ulakhan Fault. Previous temporary deployments in the vicinity of the Ulakhan fault lasted only a few days at most. In these deployments, high seismicity levels were observed, with up to ten local events per day. We conducted a more extensive deployment to verify the levels of seismic activity in the vicinity of the Ulakhan. Two short-period seismic stations were deployed a few kilometers off the main Seimchan highway and within the basin. Both stations were within 15 km of the Ulakhan fault. Although these stations were not ideally situated from a noise perspective, we recorded 84 local earthquakes (distances less than the Pn/Pg crossover distance, which is about 120 km for this area) in 33 days, with the stations having a 92% operational data collection rate. A sample seismogram of a local event is shown in Figure 5.

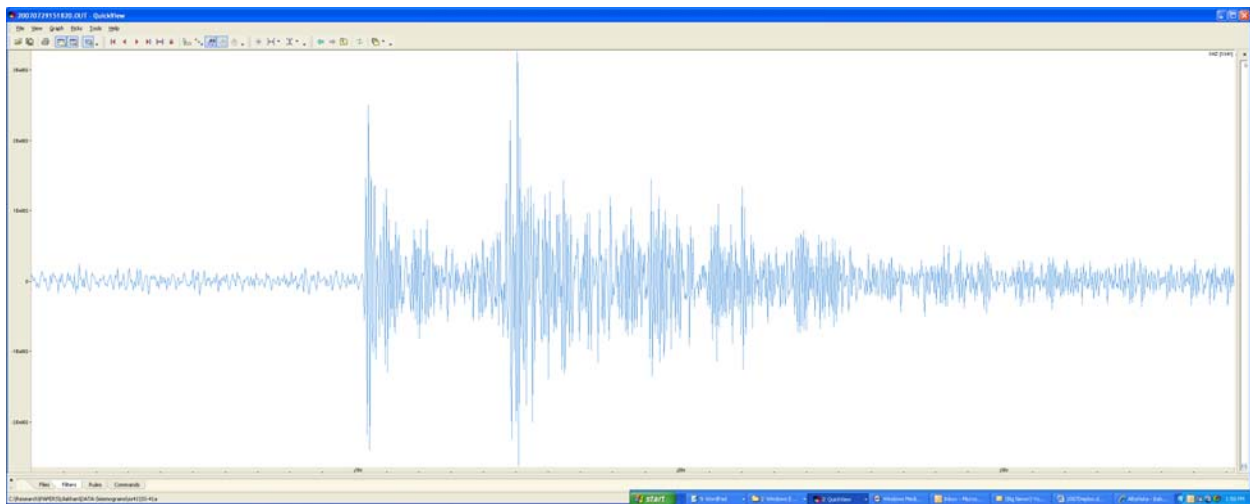


**Figure 5. Sample seismogram from one of the temporary stations deployed along the Ulakhan fault in the fall of 2007. The S-P time for this local event is about 4.5 seconds.**

In theory, the Ulakhan fault system should extend to the southeast, eventually intersecting and crossing the isthmus of Kamchatka. We have expanded our focal mechanism catalog to include northeast Kamchatka, including events in Shelikhov Bay and the enigmatic zone of seismicity north of the Kamchatka-Aleutian arc-arc junction (Figure 6).

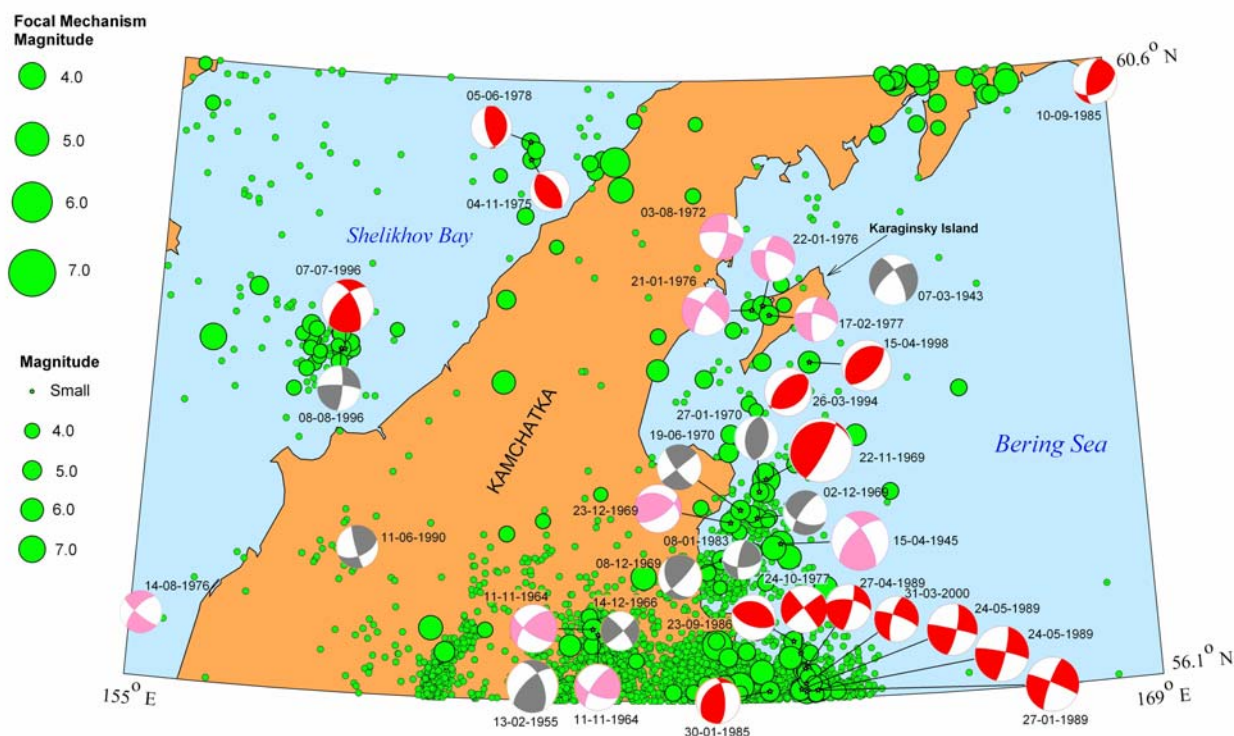


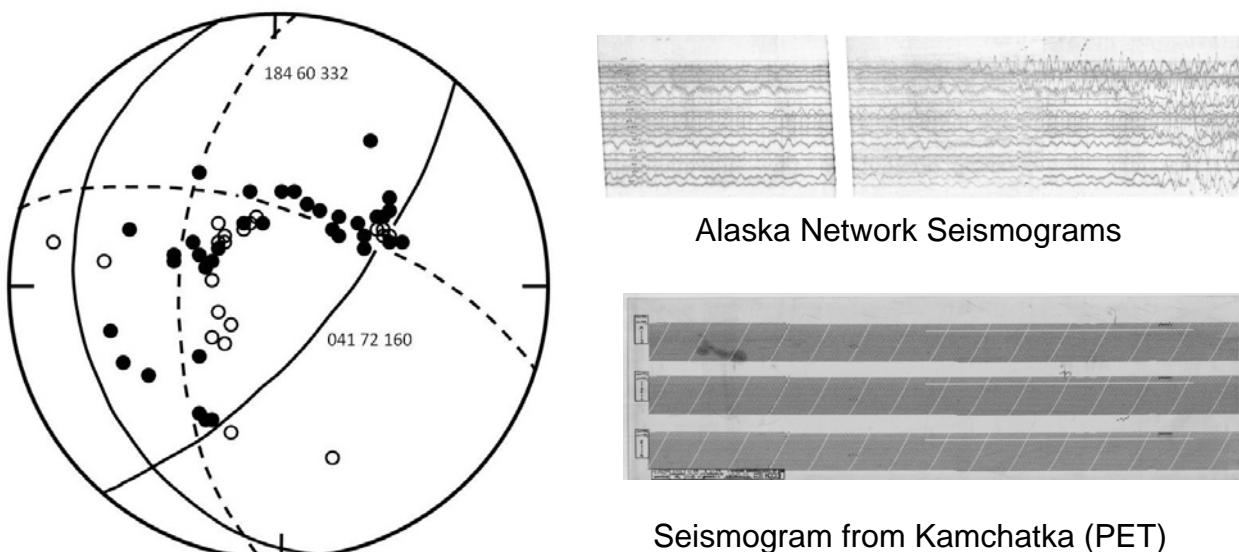
**Figure 6. Previously determined focal mechanisms presented in the literature for northeast Kamchatka. Focal mechanisms are lower hemisphere projections with compressional quadrants solid. Red mechanisms are reliable (CMT, synthetic, or well-constrained first motions), pink mechanisms are unreliable, and grey mechanisms are those for which the raw data are not available. Epicenters and focal mechanisms are scaled by magnitude.**

The distribution of seismicity and the previously determined focal mechanisms have been interpreted as representing strike-slip faulting along the Kommandorsky Islands in the southeast (Pacific-Bering plate motion), a convergence between Bering and Okhotsk north of the arc-arc junction to Karaginsky Island, thrusting between Bering and North America in the northeast, and transpression between Okhotsk and North America in the northwest (e.g., Fujita et al., 1990; Mackey et al., 1997; Pedoja et al., 2006).

Of particular interest is the cluster of events on the west side of Karaginsky Island and on the adjacent Kamchatka Isthmus. The mechanisms for this cluster shown in Figure 6 are taken from McMullen (1985) and suggest transtension—possibly with two different orientations. The Karaginsky Island sequence occurred in 1976–1977 (Zobin and Matvienko (1991) and is presumed to have had a northeast-southwest-trending rupture based on the aftershock sequence (McMullen 1985; Zobin and Matvienko, 1991). Three distinctly different mechanisms have been proposed for the events of this sequence, the transtensional mechanism (Figure 7; McMullen, 1985), a dip-slip mechanism with an approximately east-west striking nodal plane (Savostin et al., 1983; Zobin and Matvienko, 1991), and a thrust mechanism with northeast-southwest compression (Koz'min, 1984). To supplement the generally teleseismic data used in these determinations, additional first-motion data were obtained from the Alaska and Kamchatka regional networks.

The first motions are the clearest for the February 17, 1977, aftershock, and worst for the January 21, 1976, mainshock. The mainshock has an extremely emergent or precursory arrival and the first motion is extremely weak,

and probably lost at lower gain stations. Data obtained for the February 17, 1977, aftershock are more impulsive and indicate compressional first motions across Kamchatka as well as Alaska. These observations are consistent with the McMullen (1985) mechanism, however, it should be noted that the teleseismic first motions from the World Wide Standardized Seismographic Network (WWSSN) are very poor, and it is possible that the dilatational first motions in the center of the focal sphere, being at greater distances, miss the true first arrival.



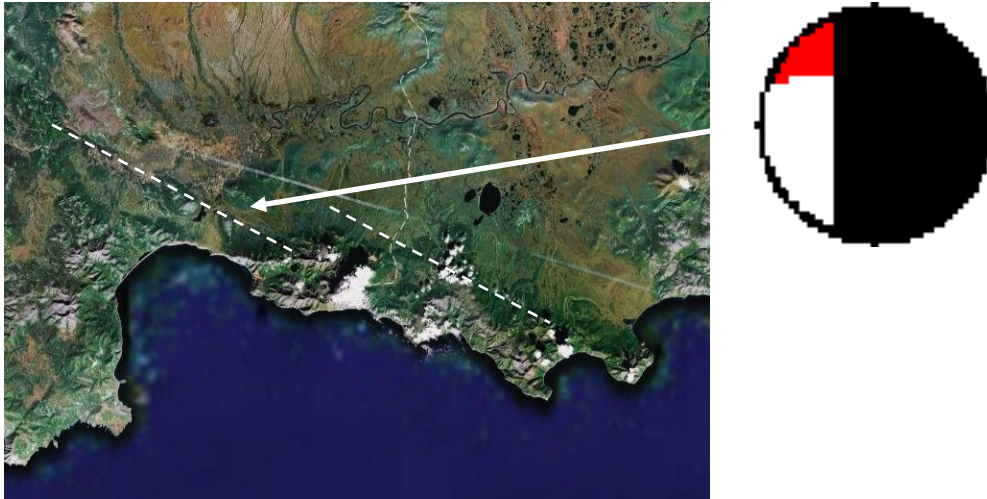
**Figure 7. Lower hemisphere projection first motion focal mechanism for the January 22, 1976, event. Solid circles are compressions, open circles are dilations. Most of the first motions are taken from the ISC bulletin except those to the southwest (Kamchatka network) and at the extreme east (Alaska network) which have been re-read (see inset for sample records). The dashed lines show the solution of McMullen (1985), while the solid lines show an alternative thrust mechanism discussed in this paper.**

Figure 7 shows the first motion focal mechanism for the January 22, 1976, aftershock. Based on the first motions, both the McMullen (1985) solution (dashed lines) and a thrust solution with northwest-southeast directed thrusting (solid lines) are possible. The thrust solution is similar to that of the large Mw 7.3 event of November 22, 1969, located just to the south. Given that the dilatations that support the transtensional solution of McMullen (1985) are from the most distant stations in Europe and south Asia, the possibility exists that the true first arrival was missed due to low-gains or attenuation. Selected WWSSN records for this event yielded no reliable first motions. Thus, the possibility that these events are subduction zone-like thrust events must be re-considered.

The first arrivals for the January 21, 1976, mainshock are complicated due to precursory arrivals (observed both on Kamchatka and Alaska regional network records) which may represent an extremely slow initiation to rupture or small, precursory events. As a result, first motion-based mechanisms for this event should be viewed with caution for this event. However, if all of the events of the Karaginsky sequence of 1976–1977 are assumed to have the same mechanism, then the data from the Kamchatka and Alaska regional networks preclude the dip-slip and thrust solutions of Savostin et al. (1983), Zobin and Matvienko (1991), and Koz'min (1984) for the January 21, 1976, mainshock. Further analysis, including waveform modeling, is planned to distinguish between the two other solutions (McMullen, 1985, and low-angle thrust) discussed here.

We have updated our general focal mechanism catalog for the Chersky Range both with new mechanisms, as well as corrected epicenters and magnitudes. In particular, we note that the January 7, 2001, earthquake west of Magadan, previously associated with the Chelomdzha-Yama fault, apparently lies on a smaller fault visible in satellite imagery (Figure 8). This, along with other aspects of the seismicity suggest that the Chelomdzha-Yama fault is not as important a structure as previously thought (e.g., Imaev et al., 2000) and may not be active in the present day.

This has significant implications for the sources of earthquakes and active faulting along the northern coast of the Sea of Okhotsk.



**Figure 8. Satellite image of epicentral region of January 7, 2001, earthquake showing WNW-ESE trending faults which parallel one of the nodal planes of the earthquake. The Global Moment Tensor solution is shown at right (Google Earth image).**

In a previous report (Mackey et al., 2007), observational evidence was presented for thrusting near the Stanovoi volcanic field. Although not enough data were available to determine a first-motion focal mechanism for any individual events, a composite focal mechanism was determined using Pg first-motions from local events recorded during the summer, 2006, deployment. Data from events located in clusters to the southeast of the volcanic field were tabulated separately from events elsewhere. The data from clusters southeast of the volcanic field are consistent with the focal mechanism (105 38 134) from first motion data for the mb 4.6 event of April 27, 1979, determined by Koz'min (1984). Use of all data yields a pure thrust focal mechanism of 110 37 090 (Figure 9), which is consistent with the orientation of the thrusts seen from the air. It should be noted that only a limited number of events were available for first motion data and crustal structure (and therefore take-off angles) was uncertain.

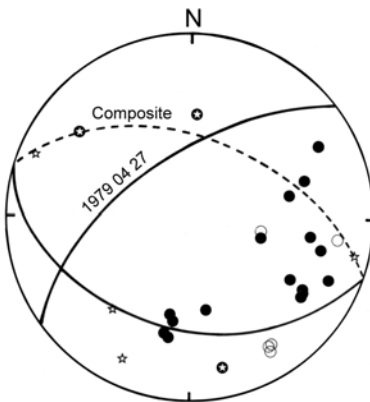


**Figure 9. Composite focal mechanism from the 2006 Stanovoi deployment. Lower hemisphere projection; compressions are solid, dilatations are open. Circles denote data from southeast of the volcanic field; stars represent other data. The solid lines show the mechanism for the April 27, 1979, event determined by Koz'min (1984), while the dashed line shows the second plane using all data from our deployment.**

**Crustal Velocities** We have extended our analysis of the eastern Russia database to conduct crustal velocity tomography for the region. Using the eastern Russia seismicity database, the epicentral ground truth of each event was evaluated using the Bondar et al. (2004) criteria and about 10–20% of our events were identified as having GT25 epicenters, that is, known to within at least 25 km of the true epicenter. GT events tend to be the largest events with highest signal-to-noise ratios and the clearest phase identifications. To invert this dataset, we used a method analogous to Pn tomography, whereby we assume a great circle path between source and receiver. Events were restricted to depths of less than 33 km, and stations were constrained to be at distances between 0.5 and 14° from the

epicenter for Pg, and 0.7 and 25° for Lg. To accommodate depth uncertainty and near-receiver velocity effects we solved for both an event term,  $e$ , and a site term,  $r$ , and we damped the site term sum to zero. The travel time for the  $i^{\text{th}}$  event to the  $j^{\text{th}}$  station is expressed as

$$t_{ij} = \sum \delta x_i s_i + e_i + r_j, \quad (1)$$

where the  $\delta x_i$  are path segments and the  $s_i$  are slownesses for those segments. The summation is taken over the  $n$  segments of the great circle path. In our solution, we employ first difference regularization over a 1° by 1° grid, and solve the set of equations using the LSQR conjugate gradient method (Paige and Saunders, 1982). We invert for slowness over a region spanned by latitudes from 45° to 75° N and longitudes from 90° to 200°E. Tests were run for checkerboards with 2°, 4°, and 10° squares with velocities alternating between  $\pm 10\%$  perturbations. Coverage with good resolution is better for Lg than for Pg largely due to the longer ray paths of Lg phases. For Lg, good resolution is obtained using 4°-grids for much of Northeastern Russia while Pg resolution is reduced.

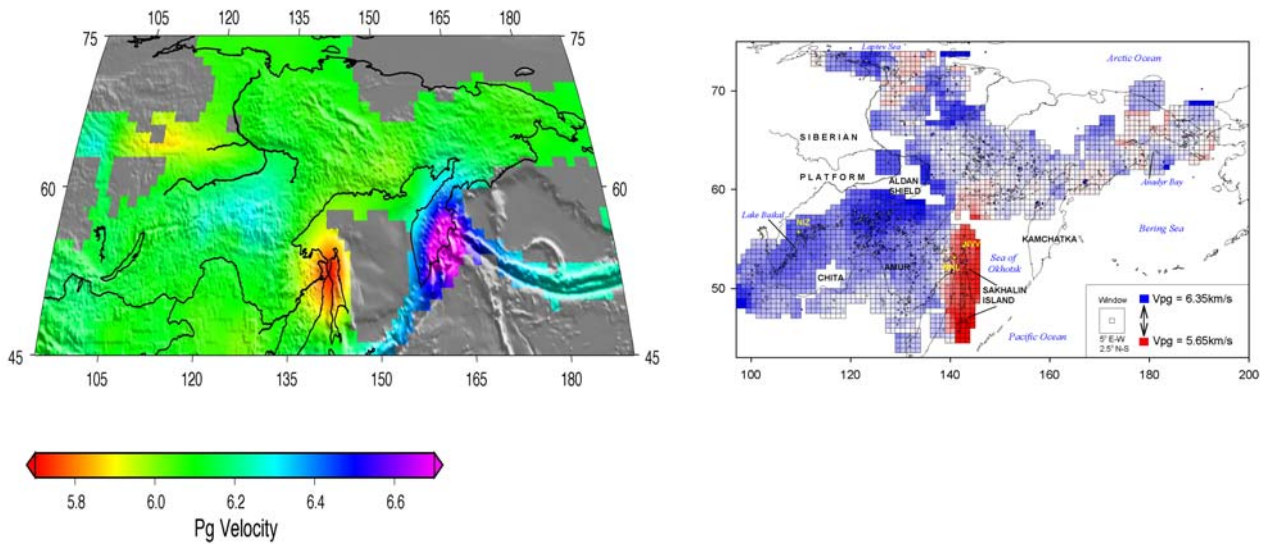


Figure 10. Left. Pg velocities of eastern Russia determined by tomography in this study. Right. Comparison of crustal velocity as determined by Mackey et al. (2003) using an independent method.

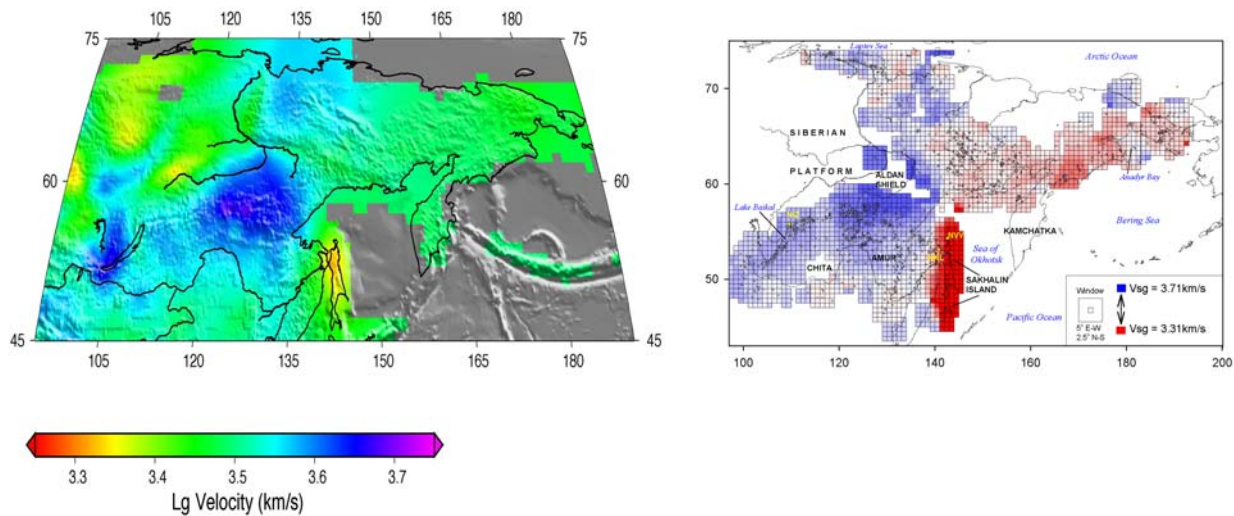
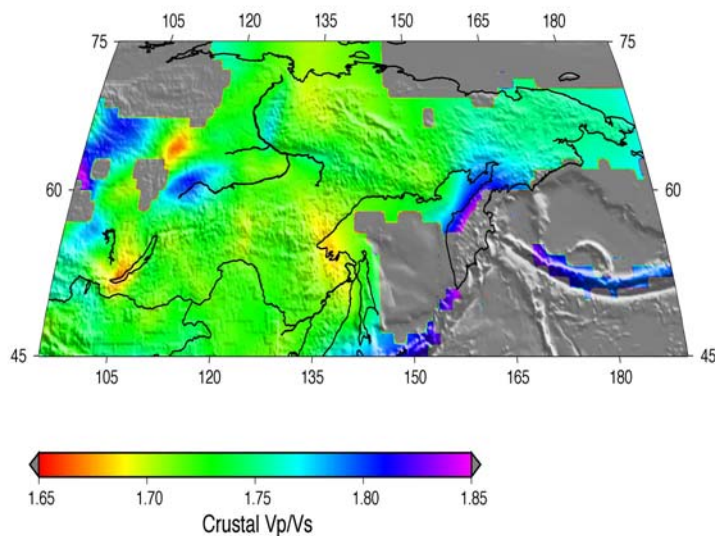


Figure 11. Left: Sg (Lg) velocities of eastern Russia determined by tomography in this study. Right: Comparison of crustal velocity as determined by Mackey et al. (2003) using an independent method.



**Figure 12. Crustal Vp/Vs ratio for eastern Russia.**

Inversion results for Pg and Lg are shown in Figures 10 and 11. Obvious trends in velocities are observed: 1) regions with convergent tectonics, i.e., the Pacific Rim, particularly associated with Kamchatka, exhibit faster than average apparent Pg velocity. 2) Sakhalin Island, where low velocities are observed. 3) The Siberian Craton (Aldan Shield), where elevated velocities are also observed, consistent with an old, thick, cold crust. We also compute Vp/Vs ratios by taking the ratio of the Pg and Lg velocity maps (Figure 12).

The tomography results can be compared with crustal velocities for eastern Russia determined several years ago by Mackey et al. (2003; Figures 10 and 11) using a method that jointly solved for seismic velocities and hypocenters while minimizing residuals. General patterns of velocity anomalies are consistent with a few exceptions. Anomalies associated with Sakhalin Island and the Aldan Shield are nearly identical in both magnitude and extent. The low velocity anomaly associated with the Laptev Sea Rift is not apparent in the tomography.

### **CONCLUSIONS AND RECOMMENDATIONS**

Traditional interpretations of faults and faulting in the area have been challenged by reanalysis of historical data and satellite image interpretation. Analysis of active faulting in conjunction with reanalysis of historical seismicity and current deployments are allowing us to improve our understanding of the nature and location of natural seismicity sources in eastern Russia. Due to the relatively low occurrence of earthquakes amenable to CMT analysis, use of historical and smaller events are critical to determining the nature of the earthquake sources. First motion data from the regional networks provide constraints which can be applied to waveform modeling and other techniques. Temporary networks provide additional information on active faulting and, as they tend to be located outside of towns, yield much lower detection thresholds.

Two independent methods have now been applied to determine Pg velocities throughout northeast Russia. While they are in general agreement, several discrepancies continue to exist and need further study. The low velocities in Sakhalin, however, have been consistent among several models and have been noted by workers of the Russian Sakhalin network as well. Careful analysis of data we are currently obtaining from Kamchatka, in particular, should improve our models of the northern Sea of Okhotsk and the northern end of the subduction zone.

The continued expansions of, and enhancements to, the MSU Siberia Seismicity database remain critical in improving both velocity models and source analysis.

### **ACKNOWLEDGEMENTS**

We would like to thank our many colleagues from the Geophysical Survey, Russian Academy of Sciences, for assistance with both data collection and fieldwork that is necessary for the continuation of this work.

**REFERENCES**

- Bondar, I, S. C. Myers, E. R. Engdahl, and E. A. Bergman (2004). Epicenter accuracy based on seismic network constraints, *Geophys. J. Int.* 156: 483–496.
- Cook, D. B., K. Fujita, and C. A. McMullen (1986). Present-day plate interactions in northeast Asia: North American, Eurasian, and Okhotsk plates, *J. Geodyn.* 6: 33–51.
- Fujita, K., D. B. Cook, H. Hasegawa, D. Forsyth, and R. Wetmiller (1990). Seismicity and focal mechanisms of the Arctic region and the North American plate boundary in Asia, in Grantz, A., G. L. Johnson, and J. F. Sweeney, J. F., eds., *The Geology of North America, v. L., The Arctic Region*, Geological Society of America, Boulder, 79-100.
- Fujita, K., G. Sella, K. G. Mackey, S. Stein, K.-D. Park, V.S. and Imaev (2004). Relationships between seismicity and GPS determined velocities in northeast Asia: *Eos Trans. Am. Geophys. Un.* 85: (47), Supplement: F667.
- Imaev, V. S., L. P. Imaeva, and B. M. Koz'min (2000). *Seismotectonics of Yakutia*, GEOS, Moscow, 226 pp. (in Russian).
- Koz'min, B. M. (1984). *Seismic Belts of Yakutia and the Focal Mechanisms of Their Earthquakes*, Nauka, Moscow, 126 pp. (in Russian).
- Mackey, K. G., K. Fujita, K., L. V. Gunbina, V. N. Kovalev, V. S. Imaev, B. M. Koz'min, and L. P. Imaeva (1997). Seismicity of the Bering Strait region: Evidence for a Bering Sea block, *Geology* 25: 979–982.
- Mackey, K. G., K. Fujita, L. K. Steck, and H. E. Hartse (2003). Seismic regionalization of eastern Russia, in *Proceedings of the 25<sup>th</sup> Seismic Research Review—Nuclear Explosion Monitoring: Building the Knowledge Base*, LA-UR-03-6029, Vol. 1, pp. 73–82.
- Mackey, K. G., H. E., Hartse, L. K. Steck, R. J. Stead, C. A. Rowe, K. Fujita, and L. Gutierrez, (2007). Seismic characterization of northeast Asia, in *Proceedings of the 29<sup>th</sup> Monitoring Research Review: Ground-Based Nuclear Explosion Technologies*, LA-UR-07-5613, Vol. 1, 123–132.
- McMullen, C. A. (1985). *Seismicity and Tectonics of the Northeastern Sea of Okhotsk*, M.S. Thesis, Michigan State University, East Lansing, 107 pp.
- Paige, C. C., and M. A. Saunders (1982). Algorithm 5583, LSQR: Sparse linear equations and least-squares problems, *Trans. Math. Software*, 8: 195-209.
- Parfenov, L. M., B. M. Koz'min, O. V. Grinenko, V. S. Imaev, and L. P. Imaeva (1988). Geodynamics of the Chersky seismic belt, *J. Geodyn.* 9: 15–37.
- Pedoja, K., J. Bourgeois, T. Pinegina and B. Higman (2006). Does Kamchatka belong to North America? An extruding Okhotsk Block suggested by coastal neotectonics of the Ozernoi Peninsula, Kamchatka, Russia, *Geology* 34: 353–356.
- Savostin, L., L. Zonenshain, and B. Baranov (1983). Geology and plate tectonics of the Sea of Okhotsk region, *Am. Geophys. Un., Geodynamics Ser.* 11: 189–221.
- Wells, D. L., and K. J. Coppersmith, (1994). New Empirical Relationships among Magnitude, Rupture Length, Rupture Width, Rupture Area, and Surface Displacement, *Bulletin of the Seismological Society of America*, 84: 974–1002.
- Zobin, V. M., and Y. D. Matvienko (1991). Karaginsky earthquake of 21(22) January, 1976, *Vulkanologiya i Seismologiya*, 13(1): 93–103. (in Russian)